

photon energies: $k_0=312$ Mev for $T=50$ Mev, and $k_0=310$ Mev for $T=125$ Mev. Also, part of the increase of the yield with increasing E_0 can be attributed to the increase in the single production due to the increase of the number of low-energy photons in the spectrum (see Fig. 5).

A computation of the cross section could be made from the yields as was done for negative pions. It would, however, be of dubious value considering the large errors which would result from the subtraction of two large quantities. Instead, we have computed the expected increase of the yield for single-pion production only. The computed single-pion yields, assumed to be equal to the observed yields at 500 Mev, are shown by the dashed curves in Fig. 10. The difference between

these curves and the experimental curves are to be attributed to pions from the pair process. From a comparison with Fig. 3 we conclude that there are about twice as many positive pions from pairs as there are negative pions. Such a result would be consistent with the assumption that the cross sections for (π^+, π^-) pairs and for (π^+, π^0) pairs were comparable.

ACKNOWLEDGMENTS

We are indebted to the staff of the Synchrotron Laboratory for its cooperation during the course of the experiment, to Professor R. F. Bacher for his interest and support, and to Professor Robert F. Christy, Dr. Jon Matthews, and Dr. F. Zachariasen for several discussions.

"Anomalous" Scattering of μ Mesons

SHUJI FUKUI, *Department of Physics, Osaka University, Osaka, Japan*

AND

TAKASHI KITAMURA AND YUZURU WATASE, *Institute of Polytechnics, Osaka City University, Osaka, Japan*

(Received August 21, 1958)

A μ -meson scattering experiment in which the mesons are required to traverse a thick block of iron and stop and decay in a thin layer of carbon, is reported. Any uncertainty in the identity of the scattered particle has thus been eliminated, and further, the momentum of the particles is well defined. The observed angular distribution of the scattered μ mesons in the momentum range $(1_{-0.2}^{+0.15})$ Bev/c has been found to be in good agreement with the distribution predicted from the Coulomb scattering theory for extended nuclei obtained by Cooper and Rainwater. There is thus no indication from the present experiment for any anomalous scattering of μ mesons near 1 Bev/c momentum.

The angular distribution of scattering of those particles which traversed the iron absorber but did not necessarily stop and decay in the carbon layer was not in good agreement with the Cooper and Rainwater theory, there being more than the expected number of particles scattered through large angles. It is shown, however, that the predicted scattering distribution, at large angles (assuming no anomalous contribution) arises almost entirely from the scattering of particles in the 1-2 Bev/c region, and therefore is very sensitive to the assumed intensity in this region. It is concluded that the results from this part of the experiment cannot be accepted as evidence favoring the existence of anomalous scattering.

The experimental results of other authors on the scattering of energetic μ mesons are summarized and discussed. It is concluded that the evidence for anomalous interactions is not strong.

I. INTRODUCTION

THE μ meson, in its interaction with matter, is believed to behave as a heavy ($207 m_e$) electron. That is, the μ meson evidently interacts mainly through its electromagnetic field, but in addition may interact with the emission and absorption of neutrinos.¹ There are a number of experiments which support this view. Walker² has observed the knock-on electrons produced by μ mesons of energy larger than 1.5 Bev. The electrons had an energy distribution consistent with that to be

expected from electromagnetic interactions alone. Barrett *et al.*³ have observed parallel pairs of μ mesons deep underground, and have concluded that these parallel pairs would not be expected if there were other than purely electromagnetic interactions. Fitch and Rainwater⁴ have investigated the level structure of μ -mesonic atoms and their results are consistent with the assumption that the μ meson interacts only electromagnetically with nuclei. Masek and Panofsky, and Masek, Lazarus, and Panofsky⁵ have observed the

¹ For example, R. E. Marshak, *Meson Physics* (McGraw-Hill Book Company, Inc., New York, 1952), Chap. 6; B. Rossi, *High-Energy Particles* (Prentice-Hall, Inc., Englewood Cliffs, New Jersey, 1952), Chap. 4.

² W. D. Walker, Phys. Rev. **90**, 234 (1953).

³ Barrett, Bollinger, Cocconi, Eisenberg, and Greisen, Revs. Modern Phys. **24**, 133 (1952).

⁴ V. L. Fitch and J. Rainwater, Phys. Rev. **92**, 789 (1953).

⁵ G. E. Masek and W. K. H. Panofsky, Phys. Rev. **101**, 1094 (1956); Masek, Lazarus, and Panofsky, Phys. Rev. **103**, 374 (1956).

TABLE I. Methods used in the experimental study of μ -meson scattering.

Method	Momentum determination	Triggering method	Possible particles accepted
I	Not measured but inferred from spectrum	Prompt coincidence	μ mesons, π mesons, protons
II	Estimated from observed scattering	Prompt coincidence	μ mesons, π mesons, protons
III	Magnetic curvature	Prompt coincidence	μ mesons, π mesons, protons
IV	Range determined with thick absorber and delayed coincidence	Delayed coincidence	μ mesons only

TABLE II. Theories of Coulomb scattering of charged particles by finite thickness of scattering materials.

Author	Charged distribution	Characteristics of distribution
Molière ^a	Point nucleus	Large-angle scattering overestimated
Olbert ^b	Scattering cutoff for $\varphi > \varphi_0 = \lambda/R$	Large-angle scattering underestimated
Cooper and Rainwater ^c	Smoothed uniform nuclear model, $R = 1.2A^{1/3} \times 10^{-13}$ cm	Presumably correct

^a See reference 17.^b See reference 18.^c See reference 16.

production of μ -meson pairs by gamma rays. This process presumably involves an interaction of the photon with the electromagnetic properties of μ mesons, and a subsequent scattering of the μ mesons in the Coulomb field of the nucleus. The experimental results were in agreement with predictions based upon this mechanism of production, and so support a purely electromagnetic character of the μ meson. Finally, after the present experiment was completed, we were informed of the Columbia experiments of Garwin *et al.*⁶ in which the μ -meson g factor was found to be 2.0064 ± 0.0048 . This result, which is to be expected if the μ meson is just a heavy electron or Dirac particle,⁷ further supports the view that μ mesons do not interact anomalously.

On the other hand, there have been a large number of experiments⁸⁻¹⁵ in which the scattering of energetic μ mesons has been measured and found to be anomalously large. Several experimental methods have been used, and they are summarized in Table I. The angular distributions which in all cases have arisen from a combination of single and multiple scattering have been compared with various scattering theories. The scattering theories¹⁶⁻¹⁸ are summarized in Table II.

⁶ Garwin, Lederman, and Weinrich, *Phys. Rev.* **105**, 1415 (1957); Coffin, Garwin, Lederman, Penman, and Sachs, *Phys. Rev.* **106**, 1108 (1957).

⁷ H. Suura and E. H. Wichman, *Phys. Rev.* **105**, 1930 (1957).

⁸ M. L. T. Kannagara and G. S. Shrikantia, *Phil. Mag.* **44**, 1049 (1953).

⁹ G. D. Rochester and A. W. Wolfendale, *Phil. Mag.* **45**, 980 (1954).

¹⁰ B. Leontic and A. W. Wolfendale, *Phil. Mag.* **44**, 1101 (1954).

¹¹ George, Redding, and Trent, *Proc. Phys. Soc. (London)* **A66**, 533 (1953).

¹² W. L. Whittemore and R. P. Shutt, *Phys. Rev.* **88**, 1312 (1952).

¹³ B. McDiarmid, *Phil. Mag.* **45**, 933 (1954); **46**, 177 (1955).

¹⁴ J. L. Lloyd and A. W. Wolfendale, *Proc. Phys. Soc. (London)* **A68**, 1045 (1955).

¹⁵ Lloyd, Rössle, and Wolfendale, *Proc. Phys. Soc. (London)* **A70**, 421 (1957).

¹⁶ L. N. Cooper and J. Rainwater, *Phys. Rev.* **97**, 492 (1955).

¹⁷ G. Molière, *Z. Naturforsch.* **2a**, 133 (1947); **3a**, 78 (1948).

¹⁸ S. Olbert, *Phys. Rev.* **87**, 319 (1952); Annis, Bridge, and Olbert, *Phys. Rev.* **89**, 1216 (1953).

The scattering theory of Cooper and Rainwater takes into account the nuclear size in a manner consistent with electron scattering results.

In Table III is shown a summary of past experimental scattering experiments. Only the experiment of Amaldi *et al.*¹⁹ has reported no anomalous scattering. It is just possible, of course, that some dynamic property of the μ meson is operative only at high energies, and so would have effects unfelt in low-energy experiments (the mesonic atom experiments, for example) but would have effects felt in the higher energy scattering experiments. On the other hand, it seemed to us that there were unresolved experimental difficulties inherent in the scattering measurements. First there is the question of "beam" purity. Only a very small intensity of π mesons or protons mixed in with a much larger intensity of μ mesons could result in a badly distorted picture of the μ -meson scattering. Also, the Coulomb scattering of μ mesons depends sensitively upon their momenta, so that unless the meson momenta are well-defined, the observed scattering cannot be critically compared with prediction. For these reasons, the present study of μ -meson scattering was undertaken. The apparatus, as described in the following section, selected for scattering measurement only those particles which traversed a large thickness of iron and stopped and decayed in a thin layer of carbon. This method not only insures that scattering measurements are made only on μ mesons, but also serves to define within narrow limits ($1_{-0.2}^{+0.15}$ BeV/c) the momenta of the mesons.

II. EXPERIMENTAL ARRANGEMENT

The experimental arrangement is illustrated in Fig. 1. The upper absorber consists of iron ingots having a density of 7.0 g/cm^3 and a total thickness of one meter. Particles, incident from the atmosphere, which give nuclear activity decrease considerably in number under the iron absorber but incident μ mesons do not. The

¹⁹ E. Amaldi and G. Fidicaro, *Nuovo cimento* **7**, 535 (1950).

TABLE III. Summary of recent μ -meson scattering experiments.

Reference	Method	Scattering material	Momentum region	Minimum angle for anomalous scattering	Cross section for anomalous scattering, $\text{cm}^2/\text{nucleon}$	No. of triggering particles
19	Counter-hodoscope (sea-level)	6 cm of iron	200 Mev $< E < 320$ Mev 320 Mev $< E$	20 degrees 20 degrees	0.8×10^{-28} 0.04×10^{-28}	249 168 204 914
12	Method III in Table I (sea-level)	5 cm of lead	$0.3 \text{ BeV} \leq E \leq 3.1 \text{ BeV}$	Result consistent with distribution expected from Molière's scattering theory for point-charge nucleus		7000
11	Method I in Table I (60 m.w.e. underground)	2 cm of lead	200 Mev $> E$ 200 Mev $< E$	15 degrees	2×10^{-28} 10^{-28}	1071 (0 cm lead below chamber) 1625 (5 cm lead below chamber) 1490 (10 cm lead below chamber)
8	Nuclear emulsion (60 m.w.e. underground)	Nuclear emulsion	$100 \text{ Mev}/c < p \leq 600 \text{ Mev}/c$	7 degrees	15×10^{-28}	
10	Method I in Table I (under 1 meter of lead at sea level)	2 cm of lead	$250 \text{ Mev}/c < p$	10 degrees	1.5×10^{-28}	626 photographs
13	Method II in Table I (26 m.w.e. underground)	2 cm of lead 2.54 cm of iron	$250 \text{ Mev}/c < p \leq 1.5 \text{ BeV}/c$ $600 \text{ Mev}/c < p \leq 3 \text{ BeV}/c$ $600 \text{ Mev}/c < p \leq 3 \text{ BeV}/c$	Result consistent with distribution expected from Molière's scattering theory for point-charge nucleus		3016 traversals 17 972 traversals 18 420 traversals
14	Method III in Table I (sea-level)	50.9 g/cm ² of lead 54.7 g/cm ² of iron	$600 \text{ Mev}/c < p \leq 3 \text{ BeV}/c$ $2 \text{ BeV}/c < p \leq 15 \text{ BeV}/c$ $600 \text{ Mev}/c < p \leq 3 \text{ BeV}/c$ $2 \text{ BeV}/c < p \leq 15 \text{ BeV}/c$			1678 2581 1705 2608
15	Method III in Table I (sea-level)	1 cm of lead	$5 \text{ BeV}/c < p < 100 \text{ BeV}/c$			272
Present exp.	Method IV in Table I (under 1 meter of the iron absorber at sea level)	1 cm of lead	$p = (1_{-0.2}^{+0.15}) \text{ BeV}/c$	Result consistent with distribution expected from Cooper and Rainwater's scattering theory for extended nucleus		4012 traversals

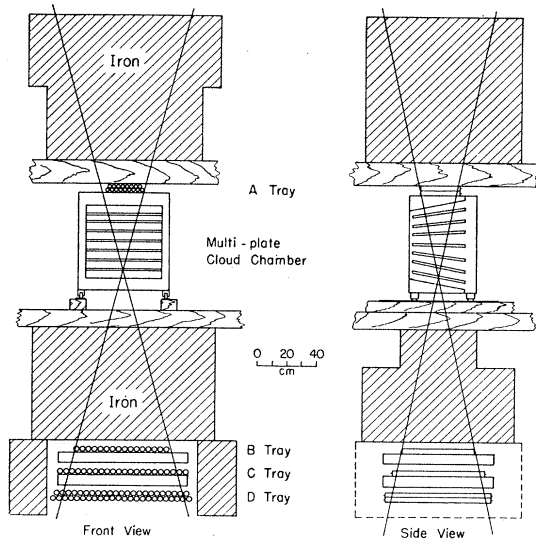


FIG. 1. Arrangement of apparatus.

cloud chamber has an effective volume of $47 \times 35 \times 50$ cm³ and contains seven one-cm-thick lead plates. The photographs were taken stereoscopically with two cameras. The axis of one camera formed an angle of 12 degrees with the axis of the chamber; the axis of the other camera was along the axis of the chamber. The 75 cm of iron below the chamber served to define the residual range of the μ mesons (momenta of 1 Bev/c). After traversing the iron, the mesons stopped and decayed in either of the two 8-cm-thick carbon slabs. Two carbon slabs, rather than just one, were used to increase the detection efficiency.

A block diagram of the circuits used in the triggering arrangement is shown in Fig. 2. The 3-cm-diameter counters in tray A were connected in parallel and thence to a common preamplifier and blocking oscillator. The counters in tray B were connected to individual preamplifiers and blocking oscillators, while the counters in tray C were separated into five groups, there being one preamplifier and blocking oscillator for each group. The counters in tray D were connected in parallel and thence to a common preamplifier and blocking oscillator. A coincidence between tray A and any one of the counters in tray B ($0.6\text{-}\mu\text{sec}$ resolving time) served to open the gates in the delay discriminator provided there was no (prompt) pulse from tray D. A delayed coincidence was recorded and the cloud chamber was triggered if there was a pulse from trays B, C, or D in the time intervals 1.3 to 3.8, 3.8 to 6.1, or 6.1 to 8.6 μsec following the AB coincidence. The large number of separate blocking oscillator circuits was required because we wished to record decay electrons in a tray through which the meson had passed before stopping.

Each counter in tray B, as well as the counters in trays C and D, were hodoscoped for the prompt pulse. Whenever a delayed coincidence occurred, neon bulbs

were photographed together with the triggered cloud chamber. In this way the track in the cloud chamber could be checked for alignment with the counters which register the event.

The cloud chamber was enclosed in a thermally insulated box in which the temperature was kept constant to $\pm 0.1^\circ\text{C}$. Distortion and track displacement were minimized through the use of a rubber expansion diaphragm to which was cemented (Cemedine No. 1500 rubber-wood glue) a piece of "Hard Board."

It is perhaps conceivable that the apparatus could be triggered by other than μ mesons. We have considered the following possibilities, all of which have been shown to have quite negligible consequences.²⁰

(I) A π meson, having been produced in a penetrating shower in the upper absorber, traverses the chamber and the lower absorber and comes to rest and decays through the $\pi\text{-}\mu\text{-}e$ process in the carbon.

(II) A π meson, produced as in (I) above, decays from within the lower absorber, the μ meson traveling on to decay in the carbon.

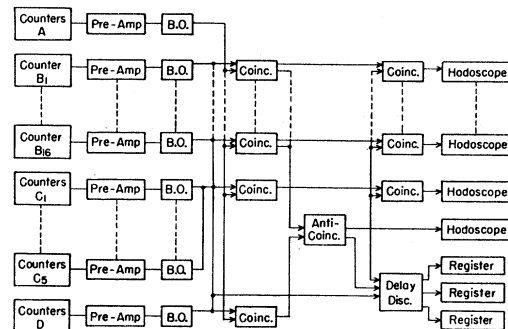


FIG. 2. Block diagram of the circuit for the triggering system.

(III) A proton incident from the atmosphere traverses the upper iron absorber to produce a π meson which goes on to decay in the carbon.

(IV) A proton incident from the atmosphere traverses the upper iron absorber and cloud chamber as in (III) above, and produces a π meson which decays within the lower absorber, the μ meson traveling on to decay in the carbon.

III. ANALYSIS OF DATA

(a) Determination of the Momentum Region of Particles in Delayed Coincidence

We estimated the band of meson momenta to which the apparatus was sensitive, taking into account (1) the momentum loss and straggling in the materials through which particles traverse, (2) the spread in the angles at which particles go through the apparatus, and (3) the uncertainty in the places at which particles stop. We obtained the value $(1_{-0.2}^{+0.15})$ Bev/c as the mo-

²⁰ T. Kitamura (to be published).

mentum region of particles selected by the delayed coincidence triggering. This value is consistent with the value estimated from the rms value of the scattering angles in the lead plates in the chamber. [See Appendix (b).] Also this value is supported by our data on the lateral distribution of the particles under the iron absorber. See Fig. 11.

(b) Data Selection

Over a period of about four months, about 900 photographs were taken with the delayed triggering requirement, and about 500 with the prompt (coincidence between trays *A*, *B*, and *D*) requirement. Only those events in which the tray *B* hodoscope records showed the discharge of one counter, or the discharge of two counters separated by one counter, or the

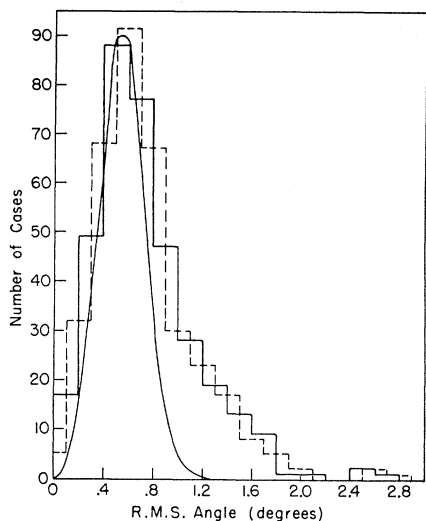


FIG. 3. Frequency plot of the rms angles of 350 tracks selected at random. The two histograms represent different groupings of the same data. The smooth curve represents Eq. (5) in McDiarmid's first paper with $p\beta = \infty$, $n = 5$, and $\sigma = 0.55$ degree.

discharge of three adjacent counters were selected for scattering analysis. The basis of this selection is discussed in Appendix (d). About 100 events were rejected because four or more counters in tray *B* were discharged. These events were evidently, for the most part, caused by side showers incident upon the apparatus. Less than half of the 100 rejected tracks gave evidence of a coincidence track within the cloud chamber. It should be emphasized that tray *B* is separated from the cloud chamber by 75 cm of iron and can hardly have introduced any appreciable basis for bias against large-angle scattering. Of the original 1400 photographs, a total of 1282 were left for analysis, there being 811 of the delayed-coincidence variety and 471 of the prompt-coincidence variety.

There were 7 lead plates in the cloud chamber. Only scattering in the central 5 plates was included in the

final analysis because distortions in the cloud chamber made measurements in the top and bottom plates unreliable. Interestingly, the scattering distribution in the top and bottom plates was accidentally consistent with the Molière (point nucleus) distribution, while, as will be discussed presently, the scattering in the central 5 plates was consistent with the Cooper and Rainwater (extended nucleus) distribution.

(c) Measurement of Scattering Angles

The images of the tracks were magnified and projected onto a stretched paper screen. The projected scattering angles of the tracks were measured to 0.1 degree. The scattering angles measured by this method were in agreement to within ± 0.3 degree with those obtained by measuring the angles directly on the film with a comparator. An uncertainty of this magnitude is quite negligible in the present experiment, and so we adopted the former method because it was faster.

(d) Measurement of Noise-Level Scattering

The root-mean-square (rms) scattering angle for high-energy particles which suffer no real scattering in the plates is called "noise-level" scattering. This noise-level scattering arises from various sources.

A track is made up of "blobs" and since these blobs are sometimes produced by low-energy gamma rays, they do not always lie along the path of the particle. Distortion such as those mentioned in connection with the top and bottom lead plates may result in apparent angular deviations, and of course there are uncertainties in the angle measurements themselves. To evaluate this noise-level scattering, we have measured the rms angles at five plates for tracks obtained with the prompt-coincidence triggering. If one of the five measured angles for any track was greater than 3.5 times the rms value for the remaining four angles, the track was excluded. According to McDiarmid,¹³ the most probable value of $\langle \theta \rangle_n$ of particles with $p \approx \infty$ is given by

$$\langle \langle \theta \rangle_n^2 \rangle_{\text{most probable}} \approx [(n-1)/n]\sigma^2,$$

where n is the number of plates traversed, θ is the projected angle, and σ is rms deviation of the noise-level scattering. The experimentally determined position of the peak in the rms noise-scattering angle distribution (see Fig. 3) serves to determine σ . The value of σ was 0.55 degree.

IV. RESULTS

The measured integral scattering distribution for 4012 lead plate traversals with delayed-coincidence triggering is shown in Fig. 4, and in Fig. 5 is shown the corresponding distribution for 2262 traversals with prompt-coincidence triggering. Only one correction has been applied to these data. The geometry of an experiment is such that there is the possibility that some

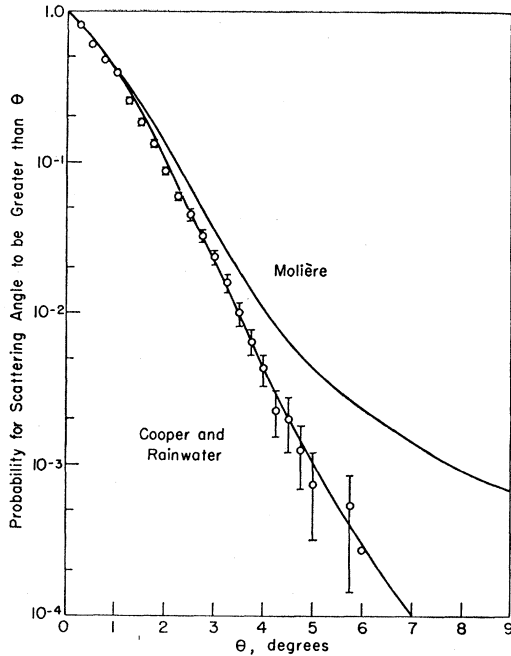


FIG. 4. Measured and calculated integral scattering distribution for particles registered by delayed coincidences. The data represent 4012 traversals of a 1-cm lead plate.

particles originally within the solid angle of the arrangement are scattered out by large-angle scattering in the lead plates, while some particles originally outside the solid angle are scattered in. These two effects tend to compensate each other, but there were residual corrections of 0, 6, and 11% for scattering angles of 5, 6, and 7 degrees, respectively. These corrections are small, and do not significantly affect our result. Nevertheless, they have been applied to the data.

The predicted distributions shown in Fig. 4 have been obtained as follows. Let $f(p\theta)$ be the (Molière, or Cooper and Rainwater) differential scattering distribution. Our experimental data cannot be compared with $f(p\theta)$ directly because the noise-level scattering tends to distort the distribution somewhat and further the particles do not have a unique value of momentum as described above. Rather, our data must be compared with a corrected distribution, $g(p\theta)$, where $g(p\theta_0)$ is given by

$$g(p\theta_0)d(p\theta_0) = \frac{d(p\theta_0)}{(2\pi)^{1/2}\sigma} \int_{-\infty}^{\infty} f(p\theta) \exp\left\{-\frac{[(p\theta_0)^2 - (p\theta)^2]}{2\sigma^2}\right\} d(p\theta),$$

where σ is the rms angle of noise-level scattering. We have plotted an integral rather than a differential distribution, and the curves shown on Fig. 4 are $G(\theta_0)$, where

$$G(\theta_0) = \int_{\theta_0}^{\infty} d\theta \int_{0.8 \text{ BeV}/c}^{1.15 \text{ BeV}/c} g(p\theta_0)S(p)d p.$$

Our data are clearly consistent with the Cooper and Rainwater distribution, and are clearly not consistent with the Molière distribution. The Molière distribution has been shown for comparison not because there is any theoretical reason to believe it is appropriate, but because as mentioned before, several past experiments have phenomenologically been in apparent agreement with it. Near 1 BeV/c, then, our data indicate that μ mesons are scattered in a manner that can be explained on a purely electromagnetic basis, and that if there is any anomalous scattering, its cross section is very small indeed.

We shall discuss next the prompt-coincidence data. The predicted scattering distribution depends upon the momentum spectrum assumed for the triggering particles, especially on the intensity of those with small momenta. The spectrum, under the upper iron absorber (1 meter thick), $S(p)$, as shown in Fig. 6, was obtained from Olbert's production spectrum at geomagnetic latitude 24° N,²¹ the energy loss in the absorber having been taken into account. The upper spectrum in the high-momentum region of Fig. 6 is that obtained by Wilson and Owen.²² The difference between these is not large enough to change our conclusions. The lower limit of the momentum, p_0 , was estimated to be 1 BeV/c as described in the previous

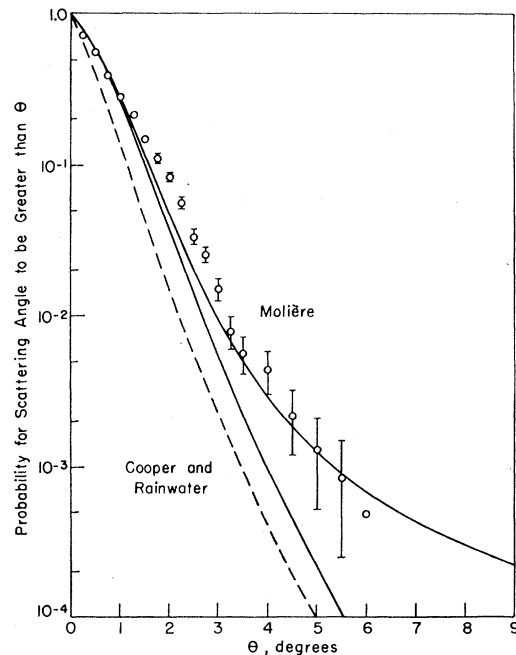


FIG. 5. Measured and calculated integral scattering distribution for particles registered by prompt coincidences. The data represent 2262 traversals of a 1-cm lead plate. The dotted curve is the uncorrected scattering distribution for the noise-level scattering.

²¹ S. Olbert, Phys. Rev. **96**, 1400 (1954).

²² J. G. Wilson and B. G. Owen, Proc. Phys. Soc. (London) **A68**, 409 (1955).

section. Then for the integral distributions we have

$$F(\theta_0) = \int_{\theta_0}^{\infty} d\theta \int_{1 \text{ Bev}/c}^{\infty} g(p\theta_0)S(p)dp,$$

and this has been plotted in Fig. 5. From this figure one sees that our prompt-coincidence data, like those of other experimenters, are consistent with the Molière distribution rather than with the Cooper and Rainwater distribution.

It would appear at first sight that our results as shown in Fig. 5 support the existence of anomalous scattering for μ mesons with momenta larger than 1 Bev/c. However, as seen in Fig. 7 which shows $g(p\theta_0)S(p)d\theta$ as a function of the angle θ_0 , the most effective momentum region for producing scattering angles greater than 4 degrees is 1–1.5 Bev/c. If we take into account possible nonuniformities in the densities of the iron absorber, the fluctuations of the momentum

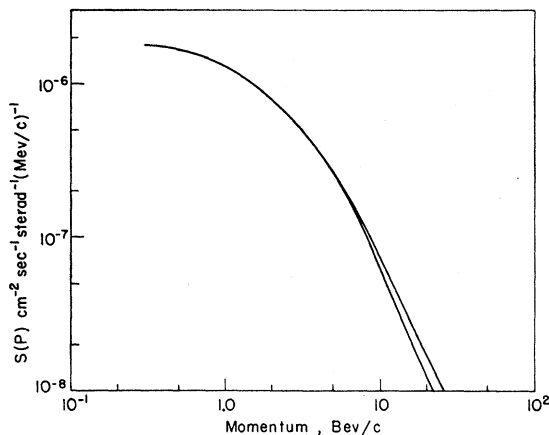


FIG. 6. The momentum spectrum of μ mesons under the one-meter-thick iron absorber. The upper spectrum in the high-momentum region is that obtained by Wilson and Owen.²²

loss, and the difference in the incident angles of particles, the value of the threshold momentum might be extended to 0.8 Bev/c. If the value of 0.8 Bev/c is accepted as the lower limit of the spectrum, the prompt-coincidence data become consistent with the Cooper and Rainwater distribution rather than with the Molière distribution as shown in Fig. 8.

It is also possible that particles other than μ mesons contribute to the prompt coincidences but not to the delayed coincidences.²⁰

V. DISCUSSION AND CONCLUSIONS

As described in Part I, the experimental results on the production of μ mesons by high-energy gamma rays seems to exclude the possibility of anomalously large μ -meson scattering at low energies. The present experiment shows that there is no anomalous scattering in the 1.0-Bev/c region, but we can say nothing definite about

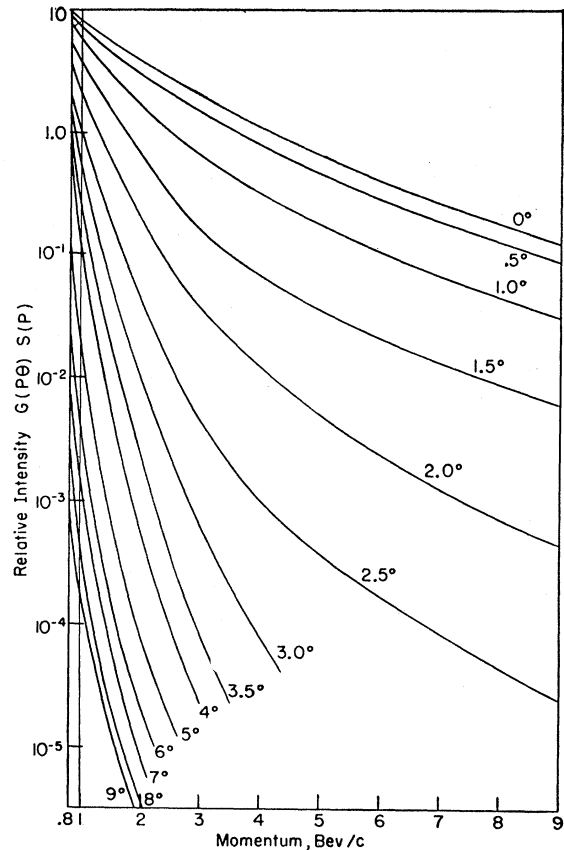


FIG. 7. The function $g(p\theta_0)S(p)d\theta$ for the present experiment.

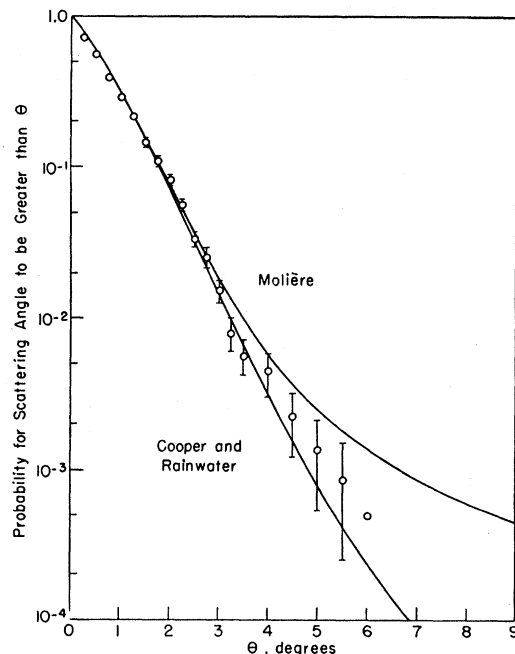


FIG. 8. Measured and calculated integral scattering distribution with the lower momentum cutoff taken to be 0.8 Bev/c for particles registered by prompt coincidence.

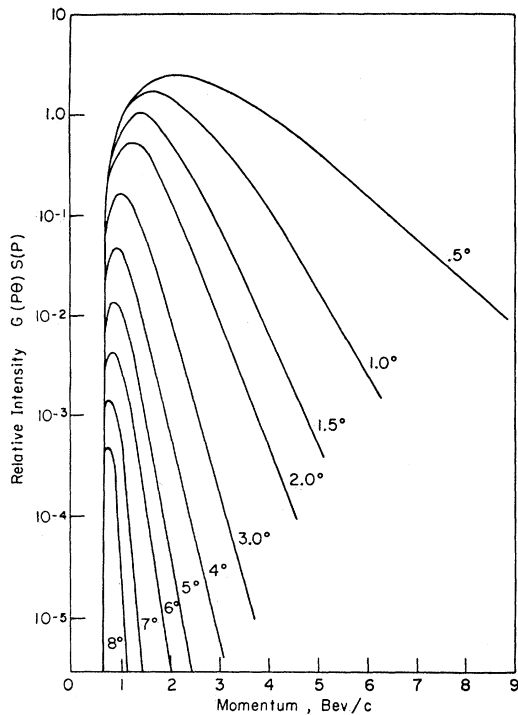


FIG. 9. The function $g(p\theta)S(p)d\phi$ for McDiarmid's experiment.

the scattering of μ mesons of 2 Bev/ c and over. There follows a discussion of experiments which do bear on the scattering of these higher energy μ mesons.

In the experiment of McDiarmid,¹³ a multiplate cloud chamber was used at a depth of 26 meters water-equivalent underground. The meson momenta ($p\beta$) were estimated through multiple-scattering measurements in six 2-cm-thick lead plates. The $p\beta$ spectrum was divided into three groups: group I (150 Mev/ $c < p\beta < 1000$ Mev/ c), group II (300 Mev/ $c < p\beta < 2200$ Mev/ c), and group III (600 Mev/ $c < p\beta < 5$ Bev/ c). Scattering, interpreted as anomalous, was found in group III. Following the method used in analyzing our own data, we have computed the function $f(p\theta)S(p)$ for this group. For $f(p\theta)$ the Cooper and Rainwater theory was used, and for $S(p)$ we have used the spectrum given by McDiarmid (Fig. 6 in his first paper). From Fig. 9 it is clear that the scattering at large angles (>5 degrees) is, under the assumption that all scattering is electromagnetic, completely determined by the mesons in the 0.6–1.5 Bev/ c region. As discussed in Appendix (b), there is a large uncertainty in determining momenta with multiple-scattering measurements, and so we feel there is a large uncertainty in the intensity of the low-momentum mesons. Thus we feel that McDiarmid's evidence is not conclusive.

Scattering measurements, in the 2–15 Bev/ c region, have been made by Leontic and Wolfendale⁵ using a magnetic cloud chamber at sea level and by Lloyd, Rössle, and Wolfendale¹⁵ in the 5–150 Bev/ c region

using the Manchester cosmic-ray spectrograph. The main problem associated with these experiments (both of which gave evidence supporting the existence of some anomalous scattering) lies in the accuracy of the momentum determinations. It is usual in such experiments to measure the root-mean-square curvature, Δc , of high-momenta tracks when there is no magnetic field present. Corresponding to this rms curvature there is a "maximum detectable momentum." According to the data given in Wilson's book,²³ however, occasional tracks may have unexpected large apparent curvatures; a distortion which produces a curvature of 1.2 m^{-1} or less can occur in one of 40 tracks in a cloud chamber which has a measured value of 0.16 m^{-1} for Δc . In a measurement²⁴ of the μ -meson momentum spectrum in a chamber for which $\Delta c = 0.2 \text{ m}^{-1}$, we found that one track in 50 had a curvature of 1.5 m^{-1} or less. In an experiment in which very rare events are measured, it is clear that distortions of this sort can be misleading, and for this reason we feel that magnetic cloud chamber measurements of μ -meson scattering must be regarded with caution.

There is further the question of a small admixture of protons in the μ -meson "beam." There is some evidence that the elasticity of high-energy proton collisions may have a value near 0.7,²⁵ so that the absorption mean free path of protons in the atmosphere would be larger than the 200–300 g/cm² previously assumed. This has the effect of increasing the estimate of the proton intensity. Presumably the ten positively charged particles which suffered large-angle deflections in Lloyd and Wolfendale's experiment were protons.

It has recently been suggested by Fowler²⁶ that large-angle μ -meson scattering may possibly be interpreted by a mechanism which is essentially the elastic counterpart of star production by μ mesons. The reason for the apparent success of this theory is essentially the fact that he assumed a large inelastic cross section, 4 mb per lead nucleus, for the incident μ mesons having energies greater than 1 Bev to transfer an energy larger than 150 Mev to a nucleus. However, George *et al.*²⁷ have shown that the observed cross section for the production of $1p$ stars and showers by μ mesons at various depths underground is on the

²³ J. G. Wilson, *Principles of Cloud Chamber Technique* (Cambridge University Press, London, 1951), Chap. 6.

²⁴ Fukui, Kitamura, and Murata, *J. Phys. Soc. Japan* **10**, 735 (1955).

²⁵ Dobrotin, Zacepin, Nikolsky, and Hristiansen, *Suppl. Nuovo cimento* **3**, 635 (1956); *Proceedings of the Oxford Conference on Extensive Air Showers*, April, 1956 (unpublished).

²⁶ G. N. Fowler, *Nuclear Phys.* **3**, 121 (1957). Note: A preprint by Dr. B. McDiarmid, describing his study of μ -meson stars and hard showers performed by using a multiplate cloud chamber containing two large plastic scintillators, has recently come to our attention; the author suggests that the cross section for production of all interactions by μ mesons involving energy transfers of 50 Mev is $(5.6 \pm 1.1) \times 10^{-30} \text{ cm}^2/\text{nucleon}$. This finding supports our criticisms of Fowler's interpretation of the anomalous scattering of μ mesons.

²⁷ E. P. George and J. Evans, *Proc. Phys. Soc. (London)* **A68**, 835 (1955).

average $(4.6 \pm 0.5) \times 10^{-30}$ cm²/nucleon and the cross section for $0p$ -star production is only about $\frac{1}{4}$ of the above value. Therefore, the value of 4 mb for the inelastic cross section seems too large. Moreover, although Fowler argued that the cross section for producing stars and showers rises fairly rapidly above 10 Bev and may become larger than 4 mb, a study of underground hard showers in our laboratory^{28,29} has shown that secondary high-energy π mesons produced by μ mesons serve to increase the apparent cross section for μ -meson showers and the genuine inelastic cross section for μ mesons is smaller than from the observed value. This results in a decrease of the anomaly discussed by Fowler, and his interpretation, we feel, is somewhat questionable.

It is thus hard to draw a very definite conclusion about the existence of the anomalous scattering for μ mesons with energies greater than 2 Bev from the experiments and theories to date as discussed above.

ACKNOWLEDGMENTS

The authors wish to express their thanks to Professor W. L. Kraushaar of the Massachusetts Institute of Technology, who had stayed in this laboratory as a Fulbright Fellow, for his early suggestion of this approach and his help in constructing the apparatus. He further gave invaluable assistance in the preparation and publication of this manuscript.

They are also indebted to the Underground Group in this laboratory and Professor S. Hayakawa of Kyoto University for their discussion and criticism. Thanks are also due to Mr. Y. Murata of the University of Tokyo who had participated in this plan, and to Mr. H. Nishimura and Mr. M. Teranaka for their invaluable assistance in carrying out this experiment. This study was supported by a Grant in Aid for Fundamental Scientific Research (Institutional Research) from the Ministry of Education in Japan.

APPENDIX

As discussed in Sec. III, our apparatus when triggered by delayed coincidences selected only μ mesons with momenta 1 Bev/c or equivalently selected only μ mesons which, when passing through the cloud chamber, had a residual range of 525 g/cm². We shall discuss here the mean life of the triggering particles, their momenta as estimated from measurements of their rms scattering angles, and their lateral displacement and angular distribution as caused by their multiple Coulomb scattering in traversing the 525 g/cm² of iron absorber.

(a) Mean Life of Triggering Particles

The decay time of the particles triggering the apparatus was obtained by using a three-channel delay

²⁸ T. Kitamura and M. Oda, Progr. Theoret. Phys. (Japan) 16, 2522 (1956).

²⁹ Higashi, Oshio, Shibata, Watanabe, and Watase (to be published).

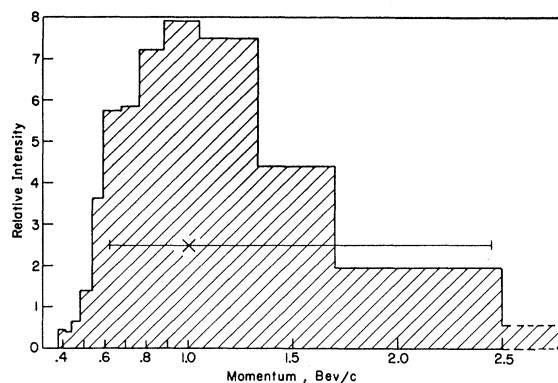


FIG. 10. Momentum distribution of particles registered by delayed coincidence. The momentum estimation was carried out by the measurement of the rms angle of multiple scattering of particles.

discriminator with gate I (1.3 to 3.8 μ sec), gate II (3.8 to 6.1 μ sec), and gate III (6.1 to 8.6 μ sec). The mean life of the triggering particles was found to be (2.1 ± 0.3) μ sec. This is in agreement with values of the mean life of μ mesons in carbon given by other workers.

(b) Estimate of Momenta by Means of the rms Scattering Angle Measurement

The momentum of a particle passing through a multiplate cloud chamber can be estimated from the rms value of the scattering angles in the plates, according to an expression obtained by Olbert.¹⁸ We have applied Olbert's method to the tracks observed with the delayed-coincidence triggering in the present experiment. The spectrum of momenta observed by the method is shown in Fig. 10, and is clearly consistent with what is to be expected.

(c) Multiple Coulomb Scattering of Particles Traversing an Absorber

When a particle passes through a thick absorber, it emerges from the absorber having suffered multiple Coulomb scattering; it travels at a deviated angle and undergoes a lateral displacement from its original direction. The angular and the lateral distributions

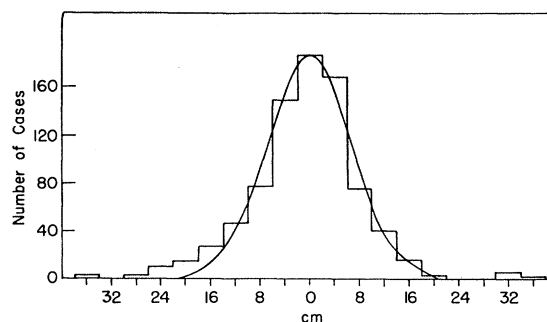


FIG. 11. The lateral distribution of particles registered by delayed coincidences. The smooth curve shows the predicted distribution of particles of 1 Bev/c.

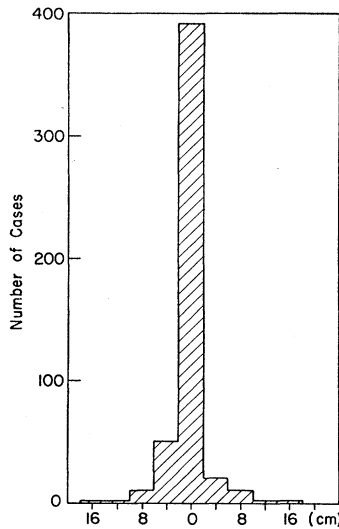


FIG. 12. The lateral distribution of particles registered by prompt coincidences.

have been given by Eyges,³⁰ taking into account an energy loss of a particle in an absorber. In the present experiment, we know the original directions of the μ -meson tracks from their cloud chamber photographs. The discrepancy between the extended direction and the position of the B -tray counter which was struck by the particle (known from the hodoscope record) provided us with the lateral displacement of the μ -meson track. The residual range of the particle after traversal of the iron absorber has an uncertainty between 0 cm and 16 cm of carbon. For simplicity, we assumed the value 120 Mev/ c for the momentum of μ mesons emerging from the iron absorber, this corresponding to a residual range of 8 cm of carbon. The lateral displacement was then computed from the expressions given by Eyges. (The lateral displacement resulting from the angular deflection of a particle after traversal of the absorber was ignored because the distance between the

³⁰ L. Eyges, Phys. Rev. 74, 1534 (1948).

bottom of the absorber and tray B is very small.) A comparison between the theoretical curve and the frequency plot of the lateral displacement of 811 delayed-coincidence tracks is indicated in Fig. 11. This result is in excellent agreement with the fact that the momentum of the individual particles was 1 Bev/ c . For comparison, the lateral displacement distribution of prompt-coincidence particles with momentum larger than 1 Bev/ c is shown in Fig. 12.

(d) Distribution of the Number of Struck Counters in B Tray

The distribution of the number of struck counters (i.e., those which register discharges) in B -tray in the photographs adopted for the present analysis is given in Table IV. Multiple discharges in tray B arise, for the

TABLE IV. Distribution of number of counters struck in tray B .

Numbers of counters struck in tray B	Delayed coincidence	
	Frequency	Percentage for total frequency
$B=1$	730	
$B=2a^a$	57	7.0 ± 0.9
$B=2s^b$	14	1.7 ± 0.5
$B=3a^c$	10	1.2 ± 0.4

^a Events in which any two adjacent counters in tray B were struck.

^b Events in which two counters in tray B separated by one counter were struck.

^c Events in which any three adjacent counters in tray B were struck.

most part, from large-angle deflections (when the meson is about to stop in the carbon) and from the knock-on electrons which accompany high-energy μ mesons.

The probability of discharging two counters with delayed-coincidence triggering was computed to be 7.0% upon using the distribution of Eyges as described above. The probability of discharging three counters was found to be 0.5%. These percentages are in fair agreement with the experimental values given in Table IV.